Article ID: 1006-8775(2023) 02-0179-12

The Response of Anomalous Vertically Integrated Moisture Flux Patterns Related to Drought and Flood in Southern China to Sea Surface Temperature Anomaly

DONG Na (董 娜)[1, 2], XU Xiang-de (徐祥德)[2], CAI Wen-yue (蔡雯悦)[2], WANG Chun-zhu (王春竹)[3], ZHAO Run-ze (赵润泽)[2], WEI Feng-ying (魏凤英)[2], SUN Chan (孙 婵)[2, 4]

(1. Department of Atmospheric and Oceanic Sciences and Institute of Atmospheric Sciences, Fudan University, Shanghai 200438 China; 2. State Key Laboratory of Severe Weather (LASW), Chinese Academy of Meteorological Sciences, Beijing 100081 China; 3. Training Center, China Meteorological Administration, Beijing 100081 China; 4. National Satellite Meteorological Center, Beijing 100081 China)

Abstract: With the extreme drought (flood) event in southern China from July to August in 2022 (1999) as the research object, based on the comprehensive diagnosis and composite analysis on the anomalous drought and flood years from July to August in 1961-2022, it is found that there are significant differences in the characteristics of the vertically integrated moisture flux (VIMF) anomaly circulation pattern and the VIMF convergence (VIMFC) anomaly in southern China in drought and flood years, and the VIMFC, a physical quantity, can be regarded as an indicative physical factor for the "strong signal" of drought and flood in southern China. Specifically, in drought years, the VIMF anomaly in southern China is an anticyclonic circulation pattern and the divergence characteristics of the VIMFC are prominent, while those are opposite in flood years. Based on the SST anomaly in the typical draught year of 2022 in southern China and the SST deviation distribution characteristics of abnormal draught and flood years from 1961 to 2022, five SST high impact areas (i.e., the North Pacific Ocean, Northwest Pacific Ocean, Southwest Pacific Ocean, Indian Ocean, and East Pacific Ocean) are selected via the correlation analysis of VIMFC and the global SST in the preceding months (May and June) and in the study period (July and August) in 1961-2022, and their contributions to drought and flood in southern China are quantified. Our study reveals not only the persistent anomalous variation of SST in the Pacific and the Indian Ocean but also its impact on the pattern of moisture transport. Furthermore, it can be discovered from the positive and negative phase fitting of SST that the SST composite flow field in high impact areas can exhibit two types of anomalous moisture transport structures that are opposite to each other, namely an anticyclonic (cyclonic) circulation pattern anomaly in southern China and the coastal areas of east China. These two types of opposite anomalous moisture transport structures can not only drive the formation of drought (flood) in southern China but also exert its influence on the persistent development of the extreme weather.

Key words: drought in southern China in 2022; VIMFC anomaly; high impact areas of SST anomaly; anomalous moisture transport circulation pattern; typical drought and flood years

CLC number: P466 **Document code:** A

Citation: DONG Na, XU Xiang-de, CAI Wen-yue, et al. The Response of Anomalous Vertically Integrated Moisture Flux Patterns Related to Drought and Flood in Southern China to Sea Surface Temperature Anomaly [J]. Journal of Tropical Meteorology, 2023, 29(2): 179-190, https://doi.org/10.46267/j.1006-8775.2023.014

1 INTRODUCTION

China has witnessed frequent drought since ancient times. Compared with other natural disasters, drought has its distinguishing features. It occurs in a wide area and lasts for a long time, with serious impact and a certain degree of persistence and delayed effect (Huang et al. [1]; Li et al. [2]; Mishra and Singh [3]). Under the background of global warming, the accelerated water cycle and changing regional climate cause large-scale regional drought year after year, with the overall drought trend becoming more extreme in terms of its frequency, intensity, duration, and influence scope (Held and Soden [4]; Dai [5]; Singh et al. [6]). In general, the spatial distribution pattern of climate in China maintains a pattern of "north drought versus south flood". However, with the intensification of climate warming, regional climate characteristics have also changed. Some traditional arid regions, such as northwest China, are gradually becoming warm and humid (Shi et al. [7]; Yao et al. [8]; Ma et al. [9]), while the drought frequency and intensity in non-traditional arid regions have increased.

Received 2022-11-06; **Revised** 2023-02-15; **Accepted** 2023-05-15

Funding: The Second Tibetan Plateau Scientific Expedition and Research (STEP) Program (2019QZKK0105); the Science and Technology Development Fund of the Chinese Academy of Meteorological Sciences (2022KJ022); Special Fund for the Basic Scientific Research Expenses of the Chinese Academy of Meteorological Sciences (2021Z013); the Science and Technology Development Fund of the Chinese Academy of Meteorological Sciences (2022KJ021); Major Projects of the Natural Science Foundation of China (91337000)

Biography: DONG Na, M.S., primarily undertaking research on synoptic climatology.

Corresponding author: XU Xiang-de, e-mail: xuxd@cma.gov.cn

For example, the frequency of drought events in the Yangtze River basin shows a significant upward trend (Lu et al. [10]; Yan et al. [11]; Xin et al. [12]; Zhai et al. [13]; Wang and Yuan [14]).

Generally, southern China enters the flood season from May to October every year, with significant increase of rainfall during this period. However, the precipitation in southern China abnormally decreased from July to August 2022, leading to severe summer drought. During the time, the precipitation of ten provinces and municipalities, including the provinces of Sichuan, Guizhou, Hunan, Jiangxi, Zhejiang, Hubei, Jiangsu, Anhui, and the municipalities of Chongqing and Shanghai, was 20% to 80% less than that in the study period of the normal year, and the average temperature was 2–4 ℃ higher than that in the study period of the normal year. In addition, compared with the data in the same historical period since 1961, the average rainfall (178.1 mm), the average temperature (29.0 ℃), and the number of high temperature days (34.1 days) in these provinces and municipalities all set new records as the lowest, the highest and the largest metrics, respectively. The high temperature and low rainfall led to the rapid development of meteorological drought in the above regions where the average number of the days with moderate drought and above (27.9 days) was the second largest in the same historical period since 1961, second only to that of 1978 (National Climate Center, http://www.weather.com.cn/climate/2022/09/3560094.shtml, September 5, 2022).

Factors leading to drought and flood in southern China are extremely complicated. From the perspective of internal atmospheric factors, East Asian atmospheric circulation anomalies such as the north Atlantic/Arctic oscillation (Xu et al. [15]; Zuo et al. [16]), the southern hemisphere annular mode (Zheng et al. [17]; Wu et al. [18]; Zheng et al. [19]), and the west Pacific subtropical high (abbreviated as WPSH) are key factors that affect the rainfall in the Yangtze River basin. The research by Sun and Ding [20] revealed that the flood in southern China in 1999 was related to the anomaly of the large-scale circulation background. The large-scale anomalous cyclonic circulation controlled the area from eastern China to Japan, which was not conducive to the northward movement of the southwest monsoon, and then generated the precipitation distribution pattern of "south flood versus north drought". Wu et al. [21] studied the regularity of the anomalous changes in summer precipitation in southern China and found that the WPSH and the southern branch trough are the main systems affecting precipitation in the region, and that the precipitation anomaly distribution is determined by the spatial configuration and intensity variation of the two systems. Niu and Li [22] analyzed the characteristics of the severe autumn drought to the south of the Yangtze River in 2004 and the accompanying circulation anomaly and concluded that the south of the Yangtze River had always been under the control of the high pressure center, which caused the strengthening of the downdraft and therefore was not conducive to precipitation. Zhang and Duan [23] found that, during the summer drought in Jiangnan (regions south of the Yangtze River) in 2013, the western part of Jiangnan and the northern part of south China were at the divergence center of moisture flux, which was unfavorable for the accumulation of moisture and resulted in the anomalously lower net moisture input compared with that in the study period of the normal year. Peng [24] also discovered that during the high temperature and drought events in southern China in the summer of 2013 the anomalies of the subtropical high and the sea surface temperature (SST) in the Indian Ocean and the South China Sea are important external forcing conditions for the occurrence of the events. The SST anomaly in the tropics can also lead to precipitation anomaly in the tropics and trigger Rossby wave responses, thus promoting the maintenance of the subtropical high in the Western Pacific Ocean (Wang et al. [25]). In addition, Zhang et al. [26] found that the autumn precipitation in southern China is very sensitive to the dynamic response of the latitudinal position of El Niño: the East Pacific Ocean-type El Niño causes more autumn precipitation in southern China while the same region experiences less rainfall with the central Pacific Ocean-type El Niño.

The anomaly of the moisture transport is an important factor affecting the transformation of regional drought and flood pattern. In this case, all key scientific issues worth studying and exploring are as follows: Why did a severe drought occur in southern China from July to August 2022? What are the anomalous characteristics of atmospheric circulation and the moisture transport structure that lead to the severe drought in south China? Does the anomalous change of SST against the backdrop of global warming also play a significant role in the severe drought? And how does it affect the precipitation in southern China by modulating the atmospheric water cycle? When anomalous drought or flood occurs in south China, what is the teleconnection structure of the moisture transport originated from the high impact areas of the mid-lower latitude ocean and what is its changing trend? Taking the drought-affected area in southern China in 2022 as the typical region, this paper is designed to explore the moisture transport structure and the driving mechanism of SST anomaly in anomalous drought and flood years in southern China.

2 DADA AND METHODS

2.1 *Data*

In this paper, 1° × 1° global monthly average SST data in 1961 – 2022 provided by the Japanese Meteorological Agency (https://www.psl.noaa.gov/data/gridded/data.cobe.html) (Ishii et al. [27]), precipitation data of 710 basic and benchmark surface meteorological observation stations in the monthly value dataset of

China's surface meteorological elements (V3.0) provided by the National Meteorological Information Center of the China Meteorological Administration from 1961 to 2022 (http://data. cma. cn/), and global monthly reanalysis data from 1961 to 2022 provided by National Center for Environmental Prediction/National Center for Atmospheric Research (NCEP/NCAR) (https://www.esrl.noaa.gov/), such as the horizontal zonal/meridional wind of the wind field (17 layers of isobaric surface), moisture fields (8 layers of isobaric surface, to 300 hPa), and surface pressure fields, the two-meter specific humidity (Kalnay et al. [28]), were applied in the analysis.

2.2 *Methods*

2.2.1 VERTICALLY INTEGRATED MOISTURE FLUX (VIMF) AND CALCULATION METHOD OF CORRELATION VECTORS

In this paper, regulatory effects of the significant ocean warming areas on the moisture transport over the anomalous precipitation areas in southern China were discussed and the structural characteristics of the moisture transport channel related to the SST anomaly of the Pacific Ocean and the Indian Ocean were further analyzed by adopting the method of the moisture transport correlation vectors in tracking the effect of the moisture source, so as to reveal the "trajectory" of the moisture transport caused by the SST anomaly in the significant warming areas. In order to overcome the interference of false moisture below the surface of the middle- and large-size terrain area in the data, the vertical integration in this paper was carried out from the height of 300 hPa to the surface (P_s). The calculation methods for vertically integrated latitudinal moisture flux (Q_u), vertically integrated longitudinal moisture flux (Q_v), the VIMF convergence (VIMFC) (Q_{div}) and the vertically integrated moisture flux vorticity (VIMFV) (Q_{vor}) from the surface (P_s) to 300 hPa are as follows:

$$Q_u(x,y,t)=\frac{1}{g}\int_{300}^{p_s} q(x,y,p,t)\,u(x,y,p,t)\,\mathrm{d}p \quad (1)$$

$$Q_v(x,y,t)=\frac{1}{g}\int_{300}^{p_s} q(x,y,p,t)\,v(x,y,p,t)\,\mathrm{d}p \quad (2)$$

$$Q_{\mathrm{div}}=\frac{1}{g}\int_{300}^{p_s}\nabla\cdot(\boldsymbol{V}q)\,\mathrm{d}p \quad (3)$$

$$Q_{\mathrm{vor}}=\frac{1}{g}\int_{300}^{p_s}\nabla\times(\boldsymbol{V}q)\,\mathrm{d}p \quad (4)$$

where g refers to the gravitational acceleration, u and v refer to the longitudinal and latitudinal winds, and q refers to the specific humidity. P_s denotes the surface pressure, P denotes the atmospheric top pressure, and Q_u and Q_v denote the vertically integrated latitudinal and longitudinal fluxes, respectively. $\nabla\cdot$ ( ) denotes the horizontal divergence, $\nabla\times$ ( ) denotes the horizontal vorticity, and $\boldsymbol{V}$= (u, v) denotes the horizontal wind vector.

$$\vec{R}(x,y)=\vec{i}R_u(x,y)+\vec{j}R_v(x,y) \quad (5)$$

where $\vec{R}$ represents the composite correlation vector, R_u (x, y) represents the correlation coefficient field of each physical quantity and the vertically integrated latitudinal flux component Q_u, and $R_v(x,y)$ represents the correlation coefficient field of each physical quantity and the vertically integrated longitudinal flux component Q_v (Wei [29]).

The calculation methods for the regional boundary, the vertically integrated total moisture flux budget and the vertically integrated longitude and latitude budget are shown as follows. First, the vertically integrated latitudinal moisture flux (Q_u) and the vertically integrated longitudinal moisture flux (Q_v) were calculated according to Eq. (1) and Eq. (2), and then the regional boundary and the vertically integrated net moisture flux budget (VINMFB) were calculated according to the following equations,

$$Q_S=\sum_{x=\lambda_1}^{\lambda_2}Q_v(x,\varphi_1,t) \quad (6)$$

$$Q_N=\sum_{x=\lambda_1}^{\lambda_2}Q_v(x,\varphi_2,t) \quad (7)$$

$$Q_W=\sum_{y=\varphi_1}^{\varphi_2}Q_u(\lambda_1,y,t) \quad (8)$$

$$Q_E=\sum_{y=\varphi_1}^{\varphi_2}Q_u(\lambda_2,y,t) \quad (9)$$

$$Q_T=Q_W-Q_E+Q_S-Q_N \quad (10)$$

where Q_W, Q_E, Q_S, Q_N are the water vapor budget at the west, east, south and north boundaries respectively; Q_T is the net water vapor budget at the regional boundary; φ_1, φ_2, λ_1, λ_2 is the latitude and longitude corresponding to each boundary respectively.

In the context of global warming, precipitation and sea surface temperature in most parts of the world have an upward trend. In order to single out the interannual signal, the linear trend is removed from global SST and precipitation in the southern region of China.

If x_i is used to denote a climate variable with a sample size of n, and t_i is used to denote the time corresponding to x_i, a one-dimensional linear regression equation between x_i and t_i is established as follows:

$$\hat{x}_i=a+bt_i,(i=1,2,\ldots,n) \quad (11)$$

In Eq. (11), a is the regression constant and b is the regression coefficient.

The least squares estimate of the regression coefficient b and the constant a for the observed data x_i and the corresponding time t_i is

$$\begin{cases} b=\dfrac{\sum_{i=1}^{n}x_it_i-\frac{1}{n}\left(\sum_{i=1}^{n}x_i\right)\left(\sum_{i=1}^{n}t_i\right)}{\sum_{i=1}^{n}t_i^2-\frac{1}{n}\left(\sum_{i=1}^{n}t_i\right)^2} \\ a=\bar{x}-b\bar{t} \end{cases} \quad (12)$$

$$\bar{x} = \frac{1}{\mathrm{n}} \sum_{i=1}^{n} x_i, \bar{t} = \frac{1}{n} \sum_{i=1}^{n} t_i \tag{13}$$

De-trending of physical quantities

$$\mathrm{x_d} = x_i - \hat{x}_i, (i = 1, 2, ..., n) \tag{14}$$

2.2.2 OTHER METHODS

In addition to the above-mentioned methods, anomaly index calculation (Guo et al. [30]), correlation coefficients, and multiple regression calculation method (Wei [29]) were also employed in this paper to identify the contribution of influencing factors.

Moreover, all physical quantities in the paper were treated through de-trending, and the average value from 1991 to 2020 was adopted as the average value of climate (i.e., perennial value).

3 THE "STRONG SIGNAL" OF THE DYNAMIC STRUCTURE OF MOISTURE FLUX IN ARID REGIONS OF SOUTHERN CHINA

2022 and 1999 are regarded as the typical drought and flood year in southern China, respectively (Sun and Ding [20]; Chen et al. [31]; Wang et al. [32]). It can be seen from the distribution of precipitation anomaly percentages in July-August of the aforesaid two years that, in 2022, the precipitation in the south of the Yangtze River basin was 20%−60% less than that in the study period of the normal year, and that figure went down to 60% or even worse in local areas (Fig. 1a). The distribution map also shows that in 1999 the precipitation in the south of the Yangtze River basin was 20%－100% more than that in the study period of the normal year, and that figure went up to 100% or even higher in local areas (Fig. 1b). Therefore, the area (21°−31° N, 103°－122° E) was selected as the key area (hereafter referred to as "Area A") in this paper. In 2022 and 1999, the VIMF anomaly fields also presented the corresponding anomalous circulation characteristics (Fig. 1c-1d). The anticyclonic (cyclonic) circulation system was identified in Area A extending to the eastern coast and the VIMFC presented a positive (negative) anomaly, which corresponded to the negative (positive) anomaly distribution of precipitation in Area A. The results showed that the VIMF divergence in Area A was significant in drought years, which caused anomalously low precipitation and contributed to the development of drought. However, the VIMF in flood years presented the typical convergence, which led to increased anomalous precipitation and eventually flood. Based on the above comparison and analysis, the anomalous vertically integrated anticyclone circulation and the average VIMFC in Area A were taken as the indicative physical factors to study the "strong signal" of arid regions in southern China.

China is located in the strongest monsoon region in the world. During the summer monsoon, the regional moisture transport determines the moisture flux budget. The amount of the moisture flux will ultimately affect the drought/flood situation in the region. To reveal the difference of vertically integrated net moisture flux budget (VINMFB) between drought years and flood years, the box-latticework web was adopted to make a quantitative analysis on the VINMFB and the inflow or outflow of each boundary in Area A. The statistical results indicated that the correlation coefficient of VINMFB changes and the physical quantity of the VIMFC in Area A is －0.88, exceeding the significance level of 0.01 (Figure omitted) and showing a significantly negative correlation. In other words, the divergence of the VIMF in drought years is strong and the VINMFB decreases sharply, while the two factors are juts the opposite in flood years. Given the characteristics of anomalous anticyclonic circulation of the VIMF anomaly in Area A, the physical quantity of the VIMFV in Area A was further calculated and it was found that the correlation coefficient of the VIMFV and the VIMFC in Area A is −0.75, surpassing the significance level of 0.01 and also showing a significant correlation. The results confirmed that the VIMFC of Area A can be used as a key physical quantity to represent the circulation dynamical structure and the characteristics of moisture flux budget changes in the arid regions of South China. From the interannual variation characteristics of the VIMFC, VIMFV, VINMFB, and precipitation (Fig. 1e) in Area A, it can also be found that the correlation coefficients of the VIMFC, VIMFV, and VINMFB in Area A with the precipitation in the study period are －0.62, 0.41, and 0.39, respectively, higher than the significance level of 0.01 and once again exhibiting strong correlations. For this reason, it can be concluded that the VIMFC is most significantly correlated with the precipitation in the study period among the three physical factors related to the moisture flux in Area A.

The correlation distribution similar to Fig. 1a can also be obtained via the respective correlation of the VIMFC, VIMFV and VINMFB in Area A from July to August in 1961−2022 with precipitation from surface meteorological observation stations in China. As the VIMFC in Area A is significantly negatively correlated with the precipitation in the south of the Yangtze River basin, but significantly positively correlated with the precipitation in central and northeastern China, it is further confirmed that the VIMFC in Area A can be used as the key "strong signal" physical factor (indicator factor) of drought and flood in south China (Fig. 1f) while the other two elements with the opposite distribution characteristics of "north negative versus south positive" (Fig. 1g-1h) are far less correlated with the precipitation in southern China than the VIMFC.

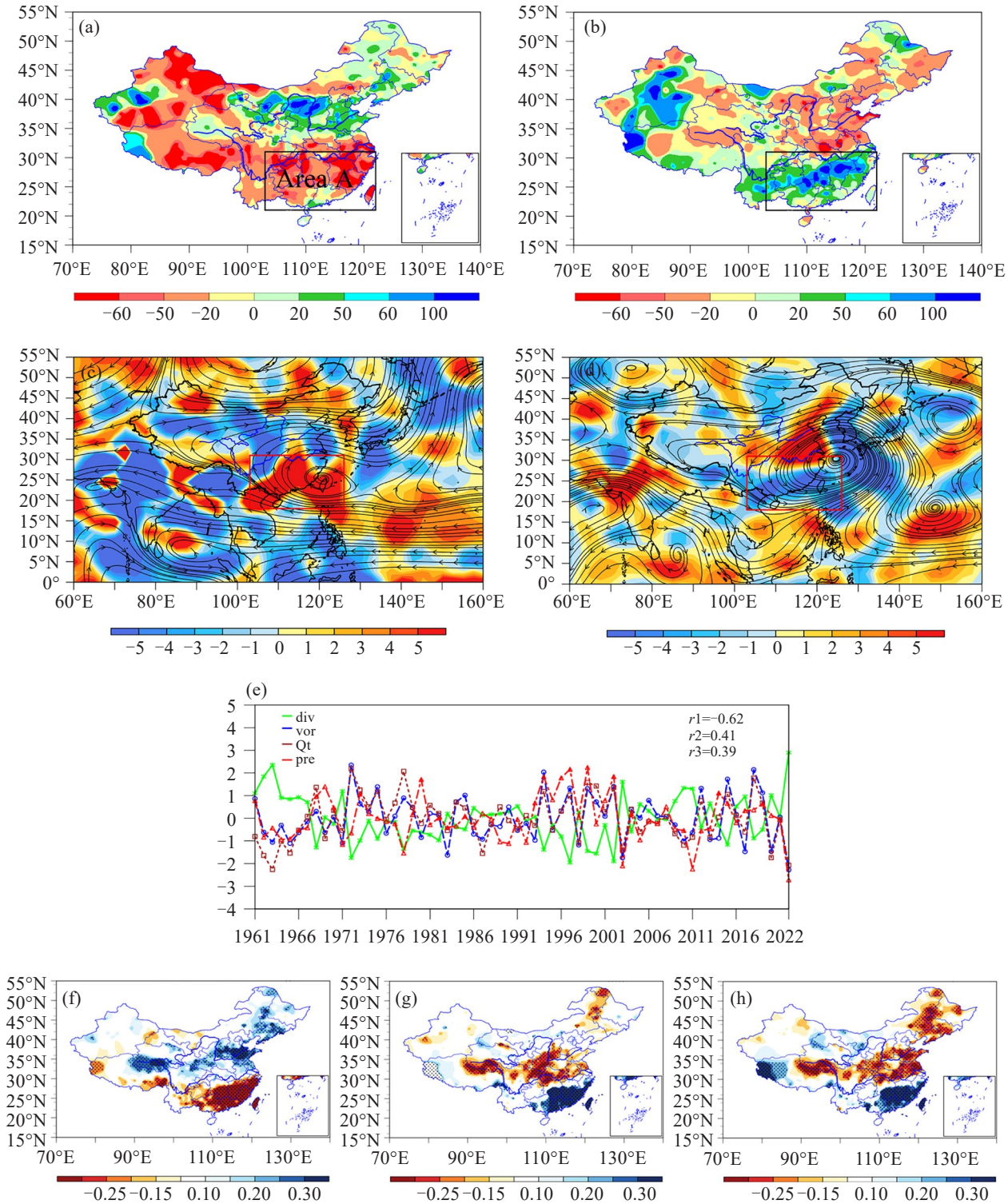

Figure 1. (a) Distribution of precipitation anomaly percentages in China during July-August of 2022 (units: %); (b) distribution of precipitation anomaly percentages in China during July-August of 1999 (units: %); (c) VIMF anomaly (units: kg m^{-1} s^{-1}) during July-August of 2022; the shadow area represents the VIMFC anomaly field (units: 10^{-5} kg s^{-1} m^{-2}); (d) VIMF anomaly (units: kg m^{-1} s^{-1}) during July-August of 1999; the shadow area represents the VIMFC anomaly field (units: 10^{-5} kg s^{-1} m^{-2}); (e) the interannual variation curves of the standardized VIMFC, VIMFV, VINMFB, and precipitation in Area A of the southern China from July to August in 1961−2022, where *r*1, *r*2, and *r*3 are the correlation coefficients of precipitation with VIMFC, VIMFV, VINMFB, respectively; and (f-h) the correlation distribution of VIMFC (f), VIMFV (g), VINMFB (h) in Area A and precipitation on the Chinese mainland during July-August of 1961−2022. (values over the 90% confidence level based on the student *t*-test are stippled).

4 ANOMALOUS MOISTURE DIVERGENCE FLOW PATTERNS IN ARID REGIONS OF SOUTHERN CHINA

In order to reveal the anomalous high - and low-level circulation configuration in typical drought and flood years in southern China, the horizontal wind anomaly flow fields at 850, 700, 500, and 300 hPa in 2022 (Fig. 2a) and 1999 (Fig. 2b) were plotted in this paper. It was demonstrated that the area of eastern China to the West Pacific Ocean is controlled by the anticyclonic (cyclonic) circulation at the low levels (850 hPa and 700 hPa), while the West Pacific Ocean anticyclonic (cyclonic) circulation extends westward and connects with the Iranian high in the west at the middle and upper levels (500 hPa and 300 hPa). The anticyclonic (cyclonic) circulation centers at different levels are all located in the east and coastal areas of southern China. The three-dimensional structure of the high and low levels in the two typical years (namely 2022 and 1999) displays similar characteristics with the circulation pattern of the VIMF anomaly field in Area A in the same year (Fig. 1c-1d). The correlation flow field of the VIMFC in Area A and the VIMF in July and August of 1961−2022 (Fig. 2c) is also similar to the anticyclonic integrated moisture flux anomaly in Area A in 2022. Therefore, it is proved that the anomalous anticyclonic (cyclonic) circulation pattern of the VIMF vector field is the critical system leading to drought (flood) in southern China.

After selecting the anomalous drought and flood years (Fig. 2d) based on the VIMFC and anomalous precipitation indexes (Guo et al. [30]) in Area A, the VIMF anomaly field in Area A in drought and flood years is synthesized (Fig. 2e-2f) and the results indicate that the VIMF in Area A in drought (flood) years is an anticyclonic (a cyclonic) anomaly circulation, and that the northward (southward) transport of moisture flow tends to be stronger in drought (flood) years, which is conducive to the moisture convergence in northern (southern) China and consequently the formation of the distribution pattern of "south drought versus north flood" ("south flood versus north drought"). Therefore, it is revealed that influenced by the East Asian summer monsoon, the anomaly circulation of the VIMF in Area A plays a key regulating role in the constant drought (flood) in southern China, reflecting the effects of the anomalous circulation dynamical structure, the moisture transport, and the moisture flux budget on drought (flood) in southern China.

To further understand the anomalies of the VIMFC, VIMFV and VINMFB triggered by the atmospheric circulation structure anomaly in the persistent drought (flood) events in southern China, we calculated the anomalies in high (1971, 2003, 2011 and 2022) and low (1994, 1997, 1999 and 2002) years of VIMFC in Area A of southern China during July-August of 1961−2002 (Table 1). The calculation results show that the typical drought (flood) event in Area A of southern China corresponds to the high (low) anomaly of the VIMFC in Area A. It is also highly correlated with the intensity of negative (positive) vorticity anomaly of the VIMF. The anticyclonic (cyclonic) dynamic structure in Area A (Fig. 2e-2f) happens to occur simultaneously with the negative (positive) VINMFB in the same area; the comprehensive analysis of the typical persistent drought (flood) event in southern China demonstrates the anomalous configuration of physical quantities of the VIMFC, VIMFV and VINMFB, all of which are identified with the two types of opposite moisture transport structures.

Table 1. Anomalies of the VIMFC (units: 10^{-5} kg s^{-1} m^{-2}), VIMFV (units: 10^{-5} kg s^{-1} m^{-2}), VINMFB (units: 10^{6} kg s^{-1}) and precipitation (units: mm) in high (1971, 2003, 2011 and 2022) and low (1994, 1997, 1999 and 2002) years of VIMFC.

Parameter	(VIMFC) MIN				(VIMFC) MAX			
YEAR	1994	1997	1999	2002	1971	2003	2011	2022
VIMFC	−2.9	−4.2	−3.1	−4.1	3.0	4.0	3.3	7.0
VIMFV	31.1	19.8	19.3	20.8	−19.3	−29.8	−11.9	−38.4
VINMFB	77.4	48.6	68.4	90.8	−31.6	−85.8	−34.7	−145.8
PRE	90.2	108.5	113.1	90.6	−77.7	−130.9	−139	−165.8

5 RESPONSE OF ANOMALOUS MOISTURE DIVERGENCE FLOW PATTERNS IN ARID REGIONS OF SOUTHERN CHINA TO THE ANOMALOUS SST IN THE HIGH IMPACT AREAS

The formation of drought (flood) is not only directly influenced by the atmospheric circulation, but also affected by external forcing factors of the climate system. Studies by Wang and Zhang [33], Li and Zhang [34] and Si et al. [35] showed that anomalies of SST in different sea areas, snow cover in Eurasia and plateaus, Antarctic and Arctic sea ice (Wu et al. [36]), and internal atmospheric factors (such as the western Pacific subtropical high and the East Asian summer monsoon) have significant influences on the location of the rain

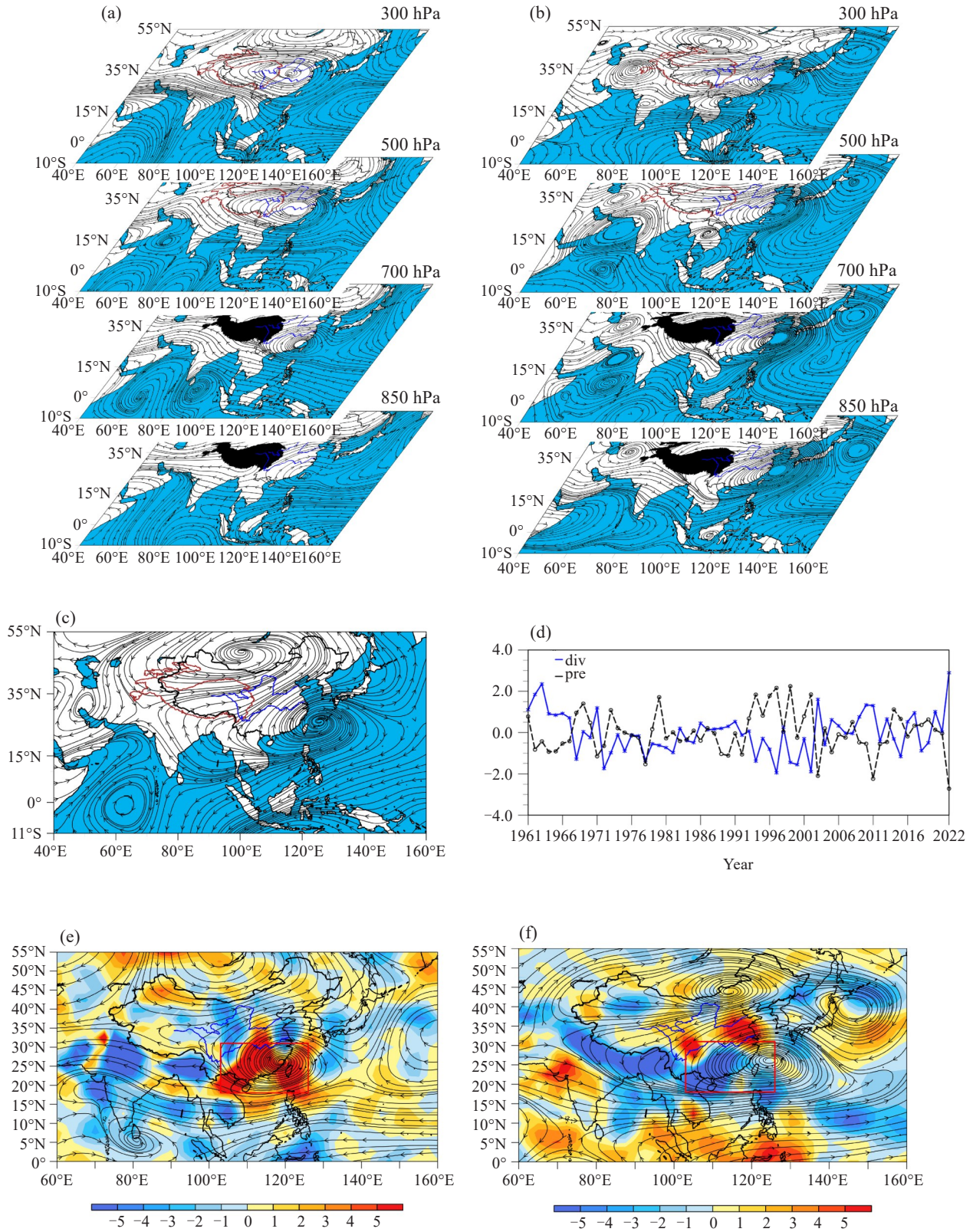

Figure 2. (a) Anomalies of flow fields at 850, 700, 500, and 300 hPa in the Asian monsoon region in July and August of 2022 (units: m s^{-1}); (b) anomalies of flow fields at 850, 700, 500, and 300 hPa in the Asian monsoon region in July and August of 1999 (units: m s^{-1}); (c) distribution of correlation between the VIMFC in Area A and the surface-300 hPa water vapor flux in July and August from 1961 to 2022; (d) the interannual variation curves of the standardized VIMFC and anomalous precipitation indexes in Area A in July and August from 1961 to 2022; (e) distribution of the composite VIMF anomaly flow field with the high (1971, 2003, 2011 and 2022) and low (f) (1994, 1997, 1999 and 2002) VIMFC values (units: kg m^{-1} s^{-1}). The shadow area denotes the anomaly field of composite VIMFC.

band and the intensity of precipitation in the same year. How does the SST change cause local climate extreme events through air-sea interaction or atmospheric wave propagation? With the purpose of finding the high impact areas of the SST anomaly closely related to drought and flood events in southern China, we selected anomalous drought and flood years according to the precipitation anomaly indexes in Area A during July to August of 1961−2022 and then took the SST composite deviation distribution of these anomalous drought/flood years (Fig. 3e) and the distribution of the global SST anomaly in July and August of 2022 (Fig. 3a) as the reference background fields. Moreover, we calculated the correlation distributions between the VIMFC in Area A and the global SST in the preceding months (May and June) and in the study period (July and August) in 1961−2022 (Fig. 3b-3c). It is found that the correlation distributions are not only similar to the distribution of the global SST anomaly (Fig. 3a) but also analogous to the distribution of the SST composite deviation (Fig. 3e). Local ocean warming might result in local water vapor anomalies. We calculated the correlation distribution between the VIMFC in Area A and the global sea-surface specific humidity in the study period (July and August) during 1961−2022 (Fig. 3d). It is found that their SST distributions are basically the same (Fig. 3b and 3d). The analysis results reveal that the SST anomalies in the preceding period (May and June) can lead to the sea-surface specific humidity anomalies in the study period (July and August), and may further affect the drought (flood) anomalies in southern China through the teleconnection pattern of water vapor transport flow. In view of the above-mentioned correlation and the distribution characteristics of the SST anomaly in Fig. 3a and Fig. 3e, five SST high impact areas (Fig. 3c) that affected the VIMFC in southern China in 2022 were selected. Among them, the North Pacific Ocean, the Northwest Pacific Ocean, the Southwest Pacific Ocean, and the Indian Ocean were positively correlated SST high impact areas, while the East Pacific was a negatively correlated SST high impact area. Moreover, the correlation coefficients of the SST sequence in May and June and those in July and August in each SST high impact area during 1961−2022 were calculated. They are 0.75, 0.73, 0.90, 0.89 and 0.94, respectively (figure omitted), which prove that the SST in each high impact area is featured with persistent anomalous change.

Meanwhile, during July-August of 1961−2022, the correlation coefficients of the VIMFC in Area A of south China and the SST of the five high impact areas in the study period are 0.48, 0.51, 0.36, − 0.26 and 0.32, respectively, all of which are higher than the significance level of 0.01, suggesting that in 2022, the above five SST high impact areas were considerably related to the VIMFC anomaly in arid Area A of southern China. Thus, what is the correlation between each SST high impact area and the VIMF anticyclonic divergence flow pattern of Area A? How much contribution does each high impact area make to the anomalous characteristics of the VIMF anticyclonic divergence flow pattern of Area A? To answer those questions, a standardized multiple linear regression equation was established with the standardized SST of the five high impact areas as the independent variable and the standardized VIMFC of Area A as the dependent variable as follows:

$$Y=0.284X_1+0.330X_2+0.061X_3-0.0561X_4+0.125X_5 \quad (15)$$

where, Y is the standardized VIMFC of Area A in July and August, and X_1-X_5 are the standardized SST in July and August of Area 1 (the North Pacific Ocean), Area 2 (the Northwest Pacific Ocean), Area 3 (the Southwest Pacific Ocean), Area 4 (the East Pacific Ocean), and Area 5 (the East Indian Ocean), respectively.

The contribution of the SST in each high impact area to the joint action of the VIMFC of Area A can be straightforwardly explained by standardized regression coefficients. From Eq. (15), it is clear that the SST regression coefficients of the five high impact areas were positive except for the East Pacific Ocean, and the fitting result was consistent with the tendency of the curve of the VIMFC in Area A. The correlation coefficient between the fitting result and the VIMFC in Area A reached 0.62 (Fig. 3f), showing that the SSTs in different high impact areas exert their influences on the anomalous VIMFC of Area A at different levels. Specifically, the west of the Northwest Pacific (Area 2) exhibited the most significant influence, with a relative contribution rate of 38%, and the relative contribution rate of the North Pacific Ocean (Area 1) is 33%. The impacts from SST Areas 5 and 3 are secondary, with relative contribution rates of 15% and 7%, respectively, while the East Pacific Ocean (Area 4) showed a relative contribution rate of − 7%. The comparison of the different contribution rates indicates that the integrated moisture transport circulation anomaly, induced by SST anomaly in the Pacific and the Indian Ocean, plays a significant role in modulating drought (flood) in southern China.

For the purpose of exploring the influence of each SST high impact area on the moisture transport in Area A, and uncovering how the structural anomaly of the moisture transport channel caused by the Pacific Ocean and Indian Ocean SST anomaly plays a regulating role in the drought in southern China, in this paper, the correlation vector calculation method between the VIMF and the SSTs in high impact areas in the preceding months (May and June) as well as in the study period (July and August) were adopted, and the correlation flow fields between the SST sequence of each high impact area and the VIMF were composited. The calculation results show that in the preceding months (May and

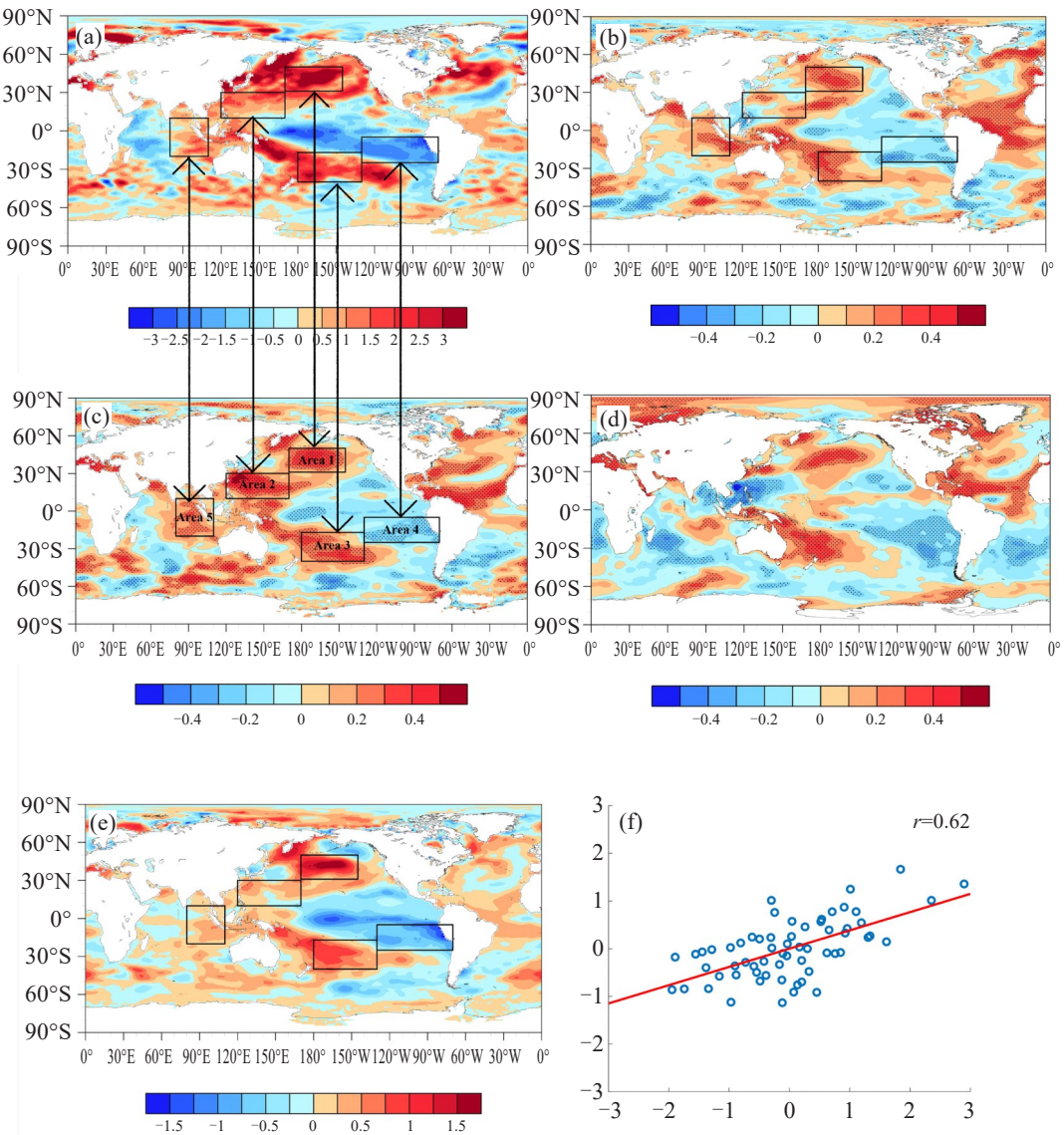

Figure 3.(a) The Global SST anomaly field in July and August of 2022 (units: ℃); (b) the correlation distribution of the VIMFC in Area A in July and August and the SST in the preceding months (May and June) from 1961 to 2022; (c) the correlation distribution of the VIMFC in Area A in July and August and the SST in the study period (July and August) from 1961 to 2022 ; (d) the correlation distribution of the VIMFC in Area A in July and August and the global sea-surface specific humidity in the study period (July and August) from 1961 to 2022, (values over the 90% confidence level based on the student *t*-test are stippled); (e) the composite deviation of SSTs in high (1971, 2003, 2011 and 2022) and low (1994, 1997, 1999 and 2002) years in Area A in July and August from 1961 to 2022; (f) correlation between the SST fitting results of high impact areas by Eq. (15) and the regional average VIMFC calculated by reanalysis data.

June), the region from Area A to the West Pacific Ocean was controlled by the anticyclonic circulation (Fig. 4a). In the study period (July and August) (Fig. 4b), the center of the anticyclonic circulation migrated westward to be located over the coastal areas of east China. Hence the region from Area A to the West Pacific Ocean was controlled by the anticyclonic circulation, which was consistent with Fig. 2c. This conclusion signals the persistent anomalous variation of the SST in each high impact area as well as its bearing on moisture transport flow pattern.

The fitting Eq. (15) was adopted to generate the correlation flow field (Fig. 4c) between the VIMF and the SST sequence in the high impact Areas 1, 2, 3 and 5, which are featured with positive contributions, as well as in Area 4 of negative contribution. Accordingly, indicative phenomenon is identified: the structure of the VIMF flow field (Fig. 4c) coincides with that of the anomaly field (anticyclonic circulation) of the VIMF in high value years (1971, 2003, 2011 and 2022) of the VIMFC (Fig. 2e). If all the coefficient symbols in the fitting Eq. (1) were reversed, the structure of the VIMF flow field (Fig. 4d) presents similar features with that of the anomaly field (cyclonic circulation) of the VIMF in low value years (1994, 1997, 1999 and 2002) of the VIMFC (Fig. 2f). This further shows that in

correspondence with the drought (flood) year in southern China, the composite flow fields of the anomalous SST in high impact areas can exhibit two types of moisture transport anomalous structures that are opposite to each other, namely the anticyclonic (cyclonic) circulation in southern China and the coastal areas in east China. The two opposite anomalous structures can drive the formation of drought (flood) in southern China and can further exert its influence on the persistent development of the extreme weather. Moreover, the SST in each high impact area is featured with persistent anomalous variation and therefore exerts persistent influence on the flow pattern of moisture transport.

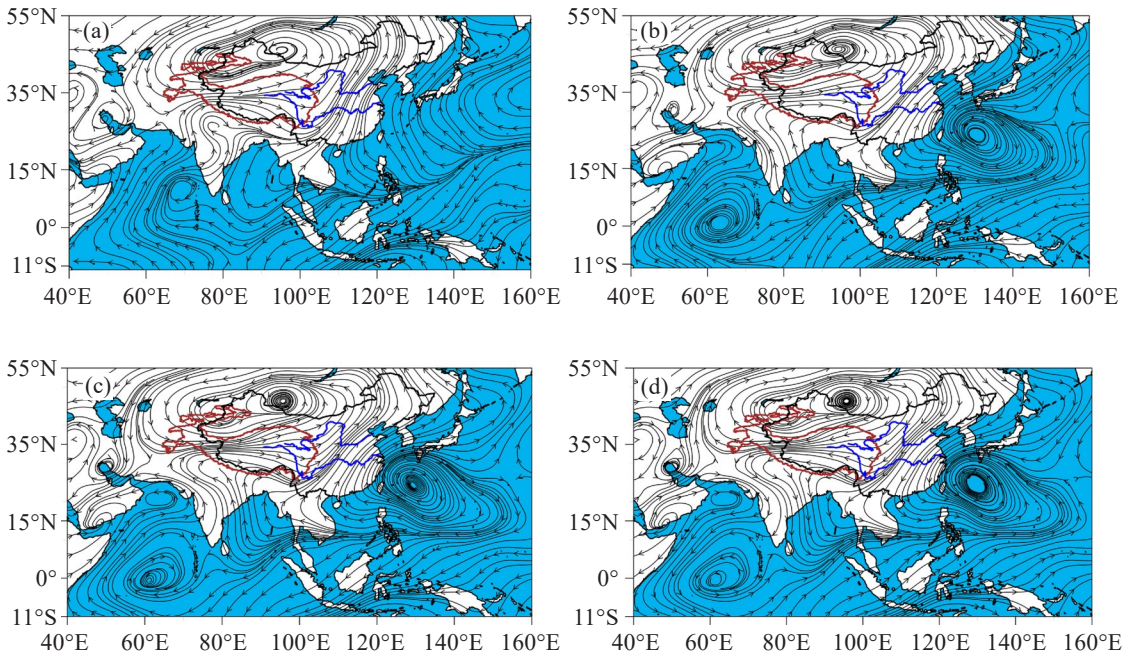

Figure 4. The composite correlation flow field between the VIMF and the SST sequence of each high impact area (a) in the preceding months (May and June) and (b) in the study period (July and August) in 1961-2022; (c) the composite correlation flow field between the VIMF and the SST sequence of each high impact area during July-August in 1961-2022; and (d) the composite correlation flow field of the VIMF and the SST sequence of each high impact area multiplied by (−1) during July-August in 1961-2022.

6 CONCLUSIONS AND DISCUSSION

In this paper, the extreme drought and flood that occurred in southern China in July and August of 1999 and 2022 were taken as typical cases, and the comprehensive diagnostic and synthetic analysis on multi-year drought and flood anomalies from 1961 to 2022 were conducted, in an attempt to analyze the structural characteristics of the anomalous moisture transport in drought and flood years in southern China, propose the indicative physical factors of the "strong signal" of drought and flood there, track the high impact areas by anomalous SSTs that play a leading role in regulating drought and flood in southern China, and reveal their modulation effect on the anomalous structure of moisture transport circulation. The conclusions were drawn as follows.

1) For the 2022 extreme drought and the 1999 extreme flood in southern China, the characteristics of the VIMF anomaly circulation pattern and the distribution characteristics of the VIMFC anomaly of the former are significantly different from those in the study period of the latter. In drought years, the VIMF anomaly in southern China is an anticyclonic circulation pattern, with significant divergence embedded in the VIMFC. In flood years, the VIMF anomaly in southern China is a cyclonic circulation pattern, and the VIMFC tends to be featured with apparent convergence. After the comparison of three physical factors related to the moisture flux, namely the VIMFC, VIMFV, and VINMFB, it is found that the correlation between the VIMFC and precipitation in the study period in southern China is the most significant. Therefore, it is proposed in this paper that the VIMFC can be used as the indicative physical factor for the "strong signal" of drought and flood in southern China.

2) The synthetic analysis on the anomaly field of the VIMF in drought and flood years in southern China in July and August of 1961−2022 shows that the typical anomaly circulation in drought (flood) years in southern China is similar to that of 2022 / 1999, with the anticyclonic or cyclonic anomaly circulation pattern, respectively, which indicates that the above two types of anomalous moisture transport circulation structures can lead to the distribution pattern of "south drought versus north drought" ("south flood versus north drought").

Our study results demonstrate that under the background of the East Asian summer monsoon, the VIMF anomaly circulation pattern plays a key regulating role in the persistent drought (flood) in southern China. The comprehensive analysis of the typical persistent drought (flood) events in southern China displays the anomalous configuration of physical quantities in the above two types of opposite moisture transport structures in the VIMFC, VIMFV and VIMNFB of the region.

3) Five SST high impact areas have been selected, namely, the North Pacific Ocean, the Northwest Pacific Ocean, the Southwest Pacific Ocean, the East Pacific Ocean and the East Indian Ocean, through the correlation analysis on the VIMFC from 1961 to 2022 and global SST in the preceding months and in the study period, based on the SST anomaly in the typical draught year of 2022 in southern China and the SST deviation distribution characteristics of abnormal draught and flood years from 1961 to 2022. In addition, the five areas' relative contributions rates to drought and flood in southern China have been quantified, indicating that the anomalous SST in the Northwest Pacific Ocean (Area 2) majorly regulates the VIMFC anomaly in southern China, with a relative contribution rate of 38%; the relative contribution rate of the North Pacific Ocean (Area 1) is 33%; The impacts from SST Areas 5 and 3 are secondary, with relative contribution rates of 15% and 7%, respectively, while SST Area 4, the East Pacific Ocean, has a relative contribution rate of − 7%. The analysis indicates that the SST in each high impact area is featured with persistent anomalous variation, which affects the flow pattern of moisture transport. Two types of anomalous moisture transport structures, which are opposite to each other, can be identified in the composite flow field of the SSTs in high impact areas, namely the anticyclonic (cyclonic) circulation anomaly in southern China and the coastal areas of east China. Through atmospheric water circulation, the two opposite anomalous structures of moisture transport can not only drive the formation of drought (flood) in southern China but also exert its influence on the persistent development of the extreme weather.

Contribution by respective authors**:** DONG Na and XU Xiang-de designed the study, performed the research and wrote the initial paper. DONG Na and CAI Wen-yue performed the statistical analyses. CAI Wen-yue, WANG Chun-zhu, ZHAO Run-ze, WEI Feng-ying, and SUN Chan contributed to subsequent revisions.

REFERENCES

[1] HUANG R H, CHEN J L, ZHOU L T, et al. Studies on the relationship between the severe climatic disasters in China and the East Asia Climate System [J]. Chinese Journal of Atmospheric Sciences, 2003, 27(4): 770-788 (in Chinese), https://doi.org/10.3878/j.issn.1006-9895.2003.04.22

[2] LI W J, ZHANG Z G, LI X, et al. The drought characteristics analysis in North China and its causes of formation [J]. Journal of Arid Meteorology, 2003, 21(4): 1-5 (in Chinese).

[3] MISHRA A K, SINGH V P. A review of drought concepts [J]. Journal of Hydrology, 2010, 391(1-2): 202-216, https://doi.org/10.1016/j.jhydrol.2010.07.012

[4] HELD I M, SODEN B J. Robust responses of the hydrological cycle to global warming [J]. Journal of Climate, 2006, 19(21): 5686-5699, https://doi.org/10.1175/JCLI3990.1

[5] DAI A G. Increasing drought under global warming in observations and models [J]. Nature Climate Change, 2013, 3(1): 52-58, https://doi.org/10.1038/nclimate1633

[6] SINGH J, ASHFAQ M, SKINNER C B, et al. Enhanced risk of concurrent regional droughts with increased ENSO variability and warming [J]. Nature Climate Change, 2022, 12(2): 163-170, https://doi.org/10.1038/s41558-021-01276-3

[7] SHI Y F, SHEN Y P, HU R J. Preliminary study on signal, impact and foreground of climatic shift from warm-dry to warm-humid in Northwest China [J]. Journal of Glaciology and Geocryology, 2002, 24(3): 219-226 (in Chinese), https://doi.org/10.7522/j.issn.1000-0240.2002.0044

[8] YAO X Y, ZHANG M J, ZHANG Y, et al. New insights into climate transition in northwest China [J]. Arid Land Geography, 2021, 45(3): 671-683 (in Chinese), https://doi.org/10.12118/j.issn.1000-6060.2021.331

[9] MA P L, YANG J H, LU G Y, et al. The transitional change of climate in the east of northwest China [J]. Plateau Meteorology, 2020, 39(4): 840-850 (in Chinese), https://doi.org/10.7522/j.issn.1000-0534.2019.00093

[10] LU E, CAI W Y, JIANG Z H, et al. The day-to-day monitoring of the 2011 severe drought in China [J]. Climate Dynamicsamics, 2014, 43(1-2): 1-9, https://doi.org/10.1007/s00382-013-1987-2

[11] YAN H, WANG S Q, WANG J B, et al. Assessing spatiotemporal variation of drought in China and its impact on agriculture during 1982−2011 by using PDSI indices and agriculture drought survey data [J]. Journal of Geophysical Research: Atmospheres, 2016, 121(5): 2283-2298, https://doi.org/10.1002/2015JD024285

[12] XIN X G, YU R C, ZHOU T J, et al. Drought in late spring of South China in recent decades [J]. Journal of Climate, 2006, 19(13): 3197-3206, https://doi. org / 10.1175/JCLI3794.1

[13] ZHAI P M, ZHANG X B, WAN H, et al. Trends in total precipitation and frequency of daily precipitation extremes over China [J]. Journal of Climate, 2005, 18(7): 1096-1108, https://doi.org/10.1175/JCLI-3318.1

[14] WANG Y M, YUAN X. The anthropogenic acceleration and intensification of flash drought over the southeastern coastal region of China will continue into the future [J]. Atmospheric and Oceanic Science Letters, 2022, 15(5): 100262, https://doi.org/10.1016/j.aosl.2022.100262

[15] XU H L, FENG J, SUN C. Impact of preceding summer North Atlantic Oscillation on early autumn precipitation over central China [J]. Atmospheric and Oceanic Science Letters, 2013, 6(6): 417-422, https://doi. org / 10.3878 / j. issn.1674-2834.13.0027

[16] ZUO J Q, REN H L, LI W J. Contrasting impacts of the arctic oscillation on surface air temperature anomalies in Southern China between early and middle-to-late winter [J]. Journal of Climate, 2015, 28(10): 4015-4026, https://

doi.org/10.1175/JCLI-D-14-00687.1

[17] ZHENG F, LI J P, LIU T. Some advances in studies of the climatic impacts of the Southern Hemisphere annular mode [J]. Journal of Meteorological Research, 2014, 28 (5): 820−835, https://doi.org/10.1007/s13351-014-4079-2

[18] WU Z W, DOU J, LIN H. Potential influence of the November-December Southern Hemisphere annular mode on the East Asian winter precipitation: A new mechanism [J]. Climate Dynamics, 2015, 44(5-6): 1215-1226, https://doi.org/10.1007/s00382-014-2241-2

[19] ZHENG F, LI J P, WANG L, et al. Cross-seasonal influence of the December-February Southern Hemisphere annular mode on March-May meridional circulation and precipitation [J]. Journal of Climate, 2015, 28(17): 6859-6881, https://doi. org / 10.1175 / JCLI-D-14-00515.1

[20] SUN Y, DING Y H. A study on physical mechanisms of anomalous activities of East Asian summer monsoon during 1999 [J]. Acta Meteorologica Sinica, 2003, 61(4): 406-420 (in Chinese), https://doi. org / 10.11676 / qxxb2003.040

[21] WU F R, CHEN S Y, KANG J F, et al. Analysis on summer precipitation anomalies and drought-flood in southern China [J]. Meteorology and Disaster Reduction Research, 2017, 40(2): 92-99 (in Chinese), https://doi.org/10.12013/qxyjzyj2017-014

[22] NIU N, LI J P. The features of the heavy drought occurring to the south of the Yangtze River in China as well as the anomalies of atmospheric circulation in autumn 2004 [J]. Chinese Journal of Atmospheric Sciences, 2007, 31(2): 254-264 (in Chinese), https://doi.org/10.3878/j.issn.1006-9895.2007.02.07

[23] ZHANG J M, DUAN L J. Characteristic and formation analysis of a persistent high temperature and drought event in Hu'nan province during summer season in 2013 [J]. Journal of Meteorology and Environment, 2018, 34 (4): 45-51 (in Chinese), https://doi. org / 10.3969 / j. issn.1673-503X.2018.04.006

[24] PENG J B. An investigation of the formation of the heat wave in southern China in summer 2013 and the relevant abnormal subtropical high activities [J]. Atmospheric and Oceanic Science Letters, 2014, 7(4): 286-290, https://doi.org/10.3878/j.issn.1674-2834.13.0097

[25] WANG B, WU R G, LI T. Atmosphere-warm ocean interaction and its impacts on Asian-Australian monsoon variation [J]. Journal of Climate, 2003, 16(8): 1195-1211, https://doi.org/10.1175/1520-0442(2003)16<1195:AOIAII>2.0.CO;2

[26] ZHANG W J, JIN F F, TURNER A. Increasing autumn drought over southern China associated with ENSO regime shift [J]. Geophysical Research Letters, 2014, 41 (11): 4020-4026, https://doi.org/10.1002/2014GL060130

[27] ISHII M, SHOUJI A, SUGIMOTO S, et al. Objective analyses of sea-surface temperature and marine meteorological variables for the 20th century using ICOADS and the Kobe Collection [J]. International Journal of Climatology, 2005, 25(7): 865-879, https://doi.org/10.1002/joc.1169

[28] KALNAY E, KANAMITSU M, KISTLER R, et al. The NCEP / NCAR 40-year reanalysis project [J]. Bulletin of the American Meteorological Society, 1996, 77(3): 437-472, https://doi. org / 10.1175 / 1520-0477(1996)077<0437:TNYRP>2.0.CO;2

[29] WEI F Y. Modern Climate Statistics Diagnosis and Prediction Technology [M]. 2nd ed. Beijing: Meteorological Press, 2007 (in Chinese).

[30] GUO Q B, XU X D, SHI X H, et al. Characteristics of winter apparent heat source in the key area of snow cover on Qinghai-Xizang Plateau and spring drought in southwest China [J]. Plateau Meteorology, 2012, 31(04): 900-909 (in Chinese).

[31] CHEN G Y, ZHANG P Q, XU L. Preliminary studies on the cause of southern flood and northern drought during the summer of 1999 in China [J]. Climatic and Environmental Research, 2001, 6(3): 312-320 (in Chinese), http://dx. doi. org / 10.3878 / j. issn. 1006-9585.2001.03.06

[32] WANG Z D, YANG Q, GONG H S, et al. Analysis of summer temperature anomaly in 1999 and 2003 in northern China [J]. Journal of Meteorology and Environment, 2006, 22(5): 6-9 (in Chinese).

[33] WANG B, ZHANG Q. Pacific-east Asian teleconnection. Part II: How the Philippine Sea anomalous anticyclone is established during El Niño development [J]. Journal of Climate, 2002, 15(22): 3252-3265, https://doi. org / 10.1175/1520-0442(2002)015<3252:PEATPI>2.0.CO;2

[34] LI C, ZHANG Q Y. The circulation characteristics of spring precipitation anomalies over the Yangtze River valley and their response to the preceding SSTA [J]. Acta Meteorologica Sinica, 2013, 71(3): 452-461 (in Chinese), https://doi.org/10.11676/qxxb2013.033

[35] SI D, YUAN Y, CUI T, et al. Anomalies of ocean and atmospheric circulation in 2013 and their impacts on climate in China [J]. Meteorological Monthly, 2014, 40 (4): 494-501(in Chinese), https://doi. org / 10.7519 / j. issn.1000-0526.2014.04.012

[36] WU B Y, ZHANG R H, WANG B, et al. On the association between spring Arctic sea ice concentration and Chinese summer rainfall [J]. Geophysical Research Letters, 2009, 36(9): L09501, https://doi. org / 10.1029 / 2009GL037299

Citation: DONG Na, XU Xiang-de, CAI Wen-yue, et al. The Response of Anomalous Vertically Integrated Moisture Flux Patterns Related to Drought and Flood in Southern China to Sea Surface Temperature Anomaly [J]. Journal of Tropical Meteorology, 2023, 29 (2): 179-190, https://doi.org/10.46267/j.1006-8775.2023.014